Differential Anticancer Drug Delivery with a Nanogel Sensitive to Bacteria-Accumulated Tumor Artificial Environment
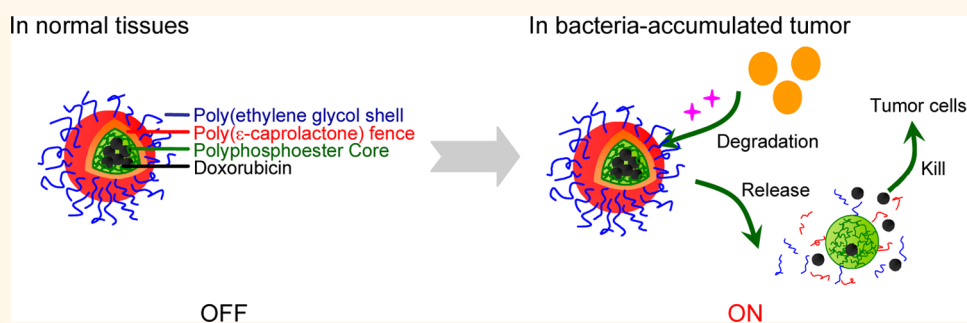
Meng-Hua Xiong,[†,§] Yan Bao,[‡,§] Xiao-Jiao Du,[‡] Zi-Bin Tan,[‡] Qiu Jiang,[‡] Hong-Xia Wang,[‡] Yan-Hua Zhu,[‡] and Jun Wang[‡,*]

[†]CAS Key Laboratory of Soft Matter Chemistry, and Department of Polymer Science and Engineering, University of Science and Technology of China, Hefei, Anhui 230026, China and [‡]CAS Key Laboratory of Brain Function and Disease, and School of Life Sciences, University of Science and Technology of China, Hefei, Anhui 230027, China. [§]These authors contributed equally.

ABSTRACT

In normal tissues → In bacteria-accumulated tumor

Poly(ethylene glycol) shell / Poly(ε-caprolactone) fence / Polyphosphoester Core / Doxorubicin

Degradation — Release — Kill — Tumor cells

OFF — ON

Differential anticancer drug delivery that selectively releases a drug within a tumor represents an ideal cancer therapy strategy. Herein, we report differential drug delivery to the tumor through the fabrication of a special bacteria-accumulated tumor environment that responds to bacteria-sensitive triple-layered nanogel (TLN). We demonstrate that the attenuated bacteria SBY1 selectively accumulated in tumors and were rapidly cleared from normal tissues after intravenous administration, leading to a unique bacteria-accumulated tumor environment. Subsequent administrated doxorubicin-loaded TLN (TLND) was thus selectively degraded in the bacteria-accumulated tumor environment after its accumulation in tumors, triggering differential doxorubicin release and selectively killing tumor cells. This concept can be extended and improved by using other factors secreted by bacteria or materials to fabricate a unique tumor environment for differential drug delivery, showing potential applications in drug delivery.

KEYWORDS: differential drug delivery · nanogel · bacteria · cancer therapy · doxorubicin

Differential delivery of anticancer agents to a tumor, which eliminates premature drug release at undesired sites but selectively releases the drug in the tumor, represents a main goal and key challenge in cancer therapy.[1−3] Strategies utilizing the unique environment of the tumor, such as redox potential, pH, or enzymes as the molecular cue to activate drug release, have received widespread attention.[3−7] However, these designs still allow for undesired activation in normal tissues, which makes it difficult to achieve differential drug delivery to a tumor *in vivo*. An alternative approach involves a system that responds to external stimuli, such as light, but this is limited by shallow tissue penetration for light.[8−12]

A unique artificial environment in a tumor, formed by the administration of exogenous material that selectively accumulates in tumors, may open up new treatment paradigms for differential anticancer drug delivery. Bacteria were studied as anticancer agents since over 1 century ago.[13−17] Today, bacterial therapies for treating cancer have re-emerged from the past and are progressing at a rapid rate.[18−22] Many different bacterial strategies have been implemented in animal models and even human trials, which have
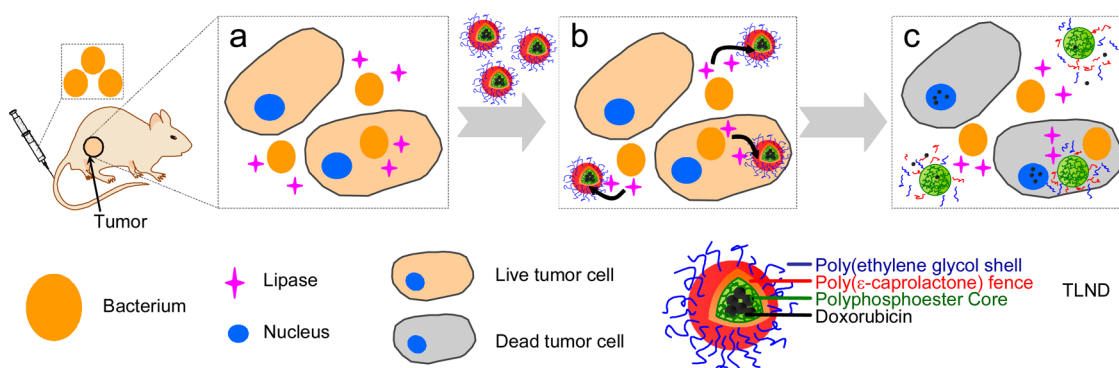
Figure 1. Doxorubicin-loaded triple-layered nanogel (TLND) for differential drug delivery to a lipase-secreting bacteria-infected tumor. By intravenous administration, lipase-secreting attenuated bacteria selectively accumulate in the tumor (a), and subsequent injection of TLND leads to its enrichment in the tumor *via* the EPR effect (b). The bacteria in the tumor selectively degrade the PCL fence of TLND to trigger DOX release and thus kill tumor cells (c).

shown experimental success, with reduced tumor volume and increased survival.[13,23] Bacterial therapies possess many unique mechanisms for treating cancer, by stimulating an immune reaction to the tumor, competing for nutrients with tumor cells, or directly killing the tumor.[13–15,19–23] Bacterial therapies have shown several advantages in cancer therapy. The genetics of bacteria can be easily manipulated, and the combination of bacteria with other cancer therapies will be crucial for creating novel strategies. For example, Cheong and co-workers have utilized the bacterial enzyme to enhance the release of liposome-encapsulated drugs within tumors, which leads to eradication of tumors.[20] Most importantly, bacteria can selectively infect and proliferate in tumors owing to the unique environment within solid tumors, including hypoxia, aberrant neovasculature, and local immune suppression.[24–26] Meanwhile, bacteria are rapidly cleared in normal tissues.[23] Thus, the administration of bacteria can fabricate a special bacteria-accumulated tumor artificial environment, which can be designed as a molecular cue for differential drug delivery.

Our previous work developed a lipase-sensitive polymeric triple-layered nanogel (TLN) for differential delivery of antimicrobials to bacterial infection sites, which shows little antibiotic release prior to reaching bacterial infection sites but rapidly releases antimicrobials once bacteria are sensed due to the degradation of the poly(ε-caprolactone) (PCL) molecular fence by the activity of bacterial lipases.[27] Here, we demonstrate that the TLN can be used as a carrier for differential anticancer drug delivery, in which drug release is in the "OFF" state in the absence of bacteria, but the drug is selectively released in response to a lipase-secreting bacteria-infected tumor environment (Figure 1). By intravenous administration of lipase-secreting attenuated bacteria into tumor-bearing mice, the bacteria preferentially enrich in the tumor but are rapidly cleared in normal tissues. Subsequent administration of anticancer drug doxorubicin (DOX)-loaded TLN (TLND) led to nanoparticle accumulation in tumors

through the enhanced permeabilization and retention (EPR) effect.[28] The bacteria selectively degrade the PCL molecular fence of TLND, triggering differential DOX release and selectively killing tumor cells.

RESULTS AND DISCUSSION

Bacteria Selectively Degrade the PCL Fence of TLND To Trigger DOX Release. TLNs are nanogel particles with an average diameter around 420 nm in water, consisting of a hydrophilic poly(ethylene glycol) shell, a cross-linked polyphosphoester core as the drug reservoir, and a degradable PCL interlayer sensitive to bacterial lipase.[27] The anticancer drug DOX was encapsulated into TLN by heating the salt form of DOX with TLN in dimethyl sulfoxide (DMSO) overnight at 60 °C, followed by the addition of water dropwise to shrink the PCL fence. The diameter of TLND was 415 nm, which was almost the same as TLN. The drug loading content was 5.98 $\pm$ 0.42%, with a fixed feeding of DOX at 50 mg mL^{-1}. The fluorescence of DOX loaded in TLND was self-quenched, corresponding to 15% of the emission intensity of DOX in water at the same concentration, due to the high local concentration of DOX in the core (Supporting Information Figure S1).[27] The enzymatic degradation in the presence of *Pseudomonas* lipase was tested by analyzing the size and count rate of TLND according to our previous work.[27] As shown in Figure S2, culturing the TLND for 24 h in Tris-HCl buffer in the absence of the enzyme did not significantly change the diameter and count rate. However, with *Pseudomonas* lipase, TLND was degraded and rapidly aggregated with notable precipitation. At the same time, the count rates continuously decreased with the increased culture time.

In this study, an attenuated strain of *Staphylococcus aureus* NCTC8325 SBY1 was used as a model bacterium, which was proved with lipase-secreting ability but with significantly reduced virulence.[29] To demonstrate selectively triggered DOX release from TLND in the presence of lipase-secreting bacteria, a 2 μL culture of green fluorescent protein-expressing SBY1 (SBY1-GFP)
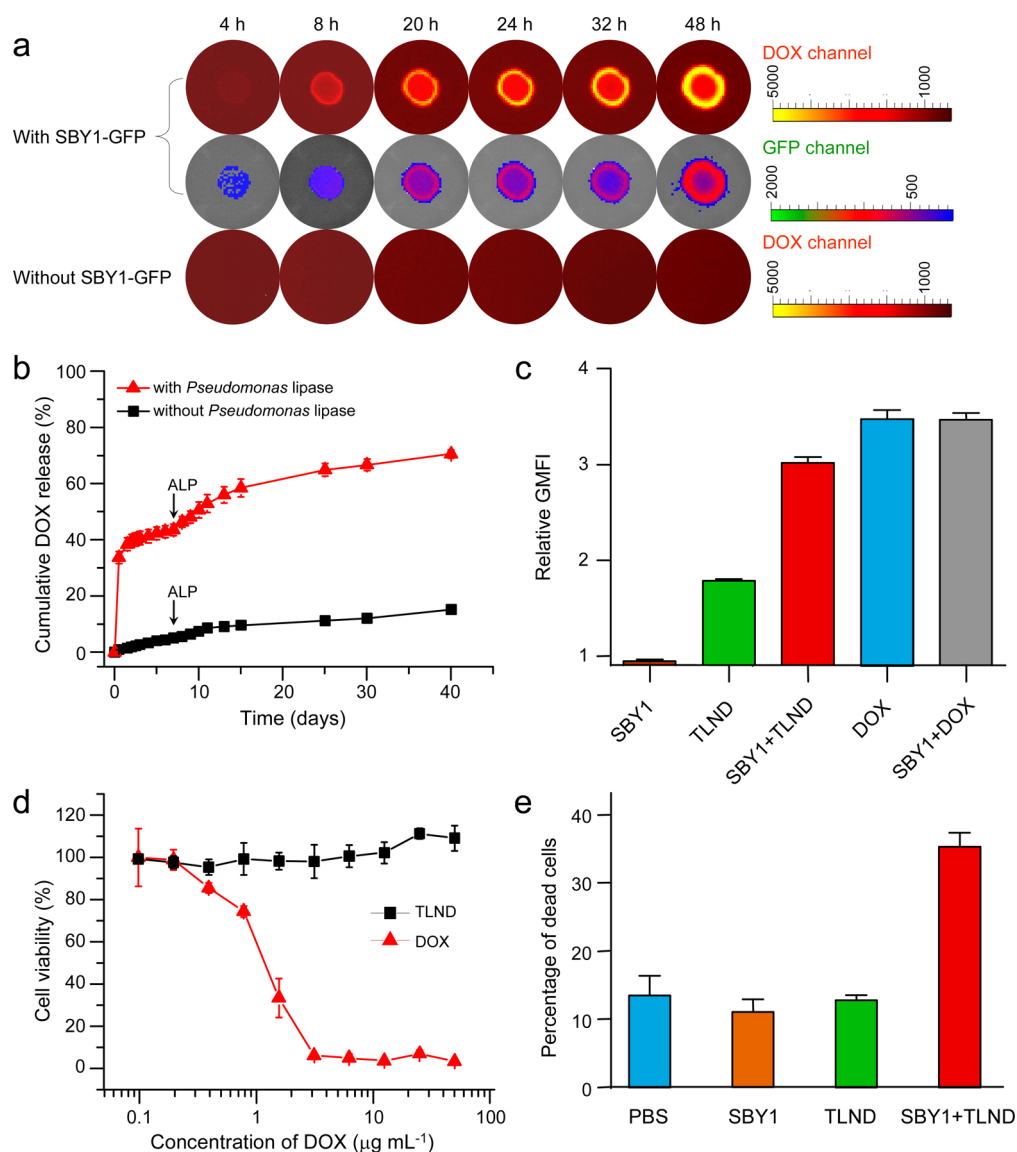
Figure 2. Lipase-secreting bacteria selectively degrade the PCL fence of TLND to trigger DOX release and selectively kill tumor cells. (a) A 2 μL culture of green fluorescent protein-expressing SBY1 (SBY1-GFP) was spotted on the center of a TSB agar plate supplemented with TLND and incubated at 37 °C. The fluorescent images of DOX and green fluorescent protein (GFP) were acquired at indicated time of incubation. **(b)** Cumulative DOX release from TLND in the absence or presence of Pseudomonas lipase. Alkaline phosphatase (ALP) was added on day 7. **(c)** Intracellular DOX fluorescence of H22 cells incubated with TLND with or without SBY1. **(d)** Cytotoxicity of DOX and TLND to H22 tumor cells analyzed by MTT assay. **(e)** Cytotoxicity of TLND to H22 tumor cells with or without SBY1 evaluated by trypan blue staining.

was spotted on the center of a TSB agar plate supplemented with TLND and incubated at 37 °C. As shown in Figure 2a, we can observe obvious zones of fluorescent recovery of DOX around the colonies of SBY1-GFP, along with the lapse of incubation time and the growth of bacteria. Further quantitative analyses of DOX fluorescence indicated 8.3 times stronger DOX fluorescence at 48 h as compared with that at 4 h in the presence of SBY1-GFP (Figure S3). On the contrary, no significant DOX fluorescence recovery was observed in the absence of SBY1-GFP. It should be noted that SBY1-GFP bacteria showed no interfering fluorescence signal in the DOX channel. The data demonstrate that the attenuated bacteria SBY1-GFP trigger DOX release from TLND.

To further reveal that bacterial-triggered DOX release is related to secreted lipase, we determined the DOX release profile in Tris-HCl buffer with or without *Pseudomonas* lipase, an enzyme known to degrade PCL.[27,30] The results shown in Figure 2b demonstrate that, without the catalyzed degradation of PCL by the lipase, DOX release was very slow, exhibiting only ~5.0% cumulative release over 7 days of incubation; no significant burst of DOX release was observed. Further addition of alkaline phosphatase (ALP) on day 7 did not accelerate the drug release rate either, though ALP is an enzyme known to catalyze the degradation of polyphosphoester,[31,32] indicating that the interaction of ALP with the polyphosphoester core was prevented

by the PCL fence. However, when TLND was incubated with *Pseudomonas* lipase, we observed rapid DOX release, reaching 33.7% of the total encapsulated amount in the first day and 43.5% in 7 days. This phenomenon could be accounted for through the destruction of the PCL fence by enzyme-catalyzed degradation. The addition of ALP on day 7 further accelerated drug release, resulting in a further 33.0% release of the total encapsulated DOX in the following 33 days. This was most likely due to the degradation of the core of TLND by ALP after the degradation of the PCL fence, which is consistent with our previous observations.[27]

Lipases are mostly secreted in the digestive system in humans, and it has been reported that lipase is secreted in a portion of human cells.[33,34] However, to the best of our knowledge, there are very limited studies that quantify exact cellular lipase concentrations. We analyzed the lipase expression in H22, HCT116 cells, hepatic cell HL-7702, and SBY1 bacterial cells. As shown in Figure S4, the lipase expression in H22 cells, HCT116 cells, and HL-7702 cells was over 10^6 times lower than that of SBY1 bacteria. Lipase expression in dead H22 cells, which were starved to death, was also very low. We also incubated H22 cells with SBY1 and collected the culture medium and lysed the cells to examine the lipase expression. The results indicated that lipase expression was significantly up-regulated with the incubation of SBY1 in both the culture medium and lysed cells. Considering that lipases are mostly secreted in the digestive system in humans and are found more abundant in bacteria,[33,34] lipase may be a good enzyme to achieve differential drug delivery. We then analyzed the fluorescence of mouse hepatoma H22 cells after coculturing TLND and SBY1 with H22 cells for 3 h (Figure 2c). Culturing the cells with TLND together with SBY1 significantly enhanced the intracellular DOX fluorescence of cancer cells, demonstrating that SBY1 triggered DOX release from TLND and resulted in a fluorescence recovery of DOX. The same phenomenon was observed in the human colorectal carcinoma HCT116 cells (Figure S5).

SBY1 Bacteria Promote the Cytotoxicity of TLND to Tumor Cells. We next evaluated the effect of SBY1 bacteria-promoted differential DOX release from TLND on tumor cell cytotoxicity. As illustrated in Figure 2d and Figure S6, TLND alone did not exhibit significant cytotoxicity to H22 cells or HCT116 cells or human normal liver HL-7702 cells at a concentration up to 50 μg mL^{-1} without the presence of SBY1, as determined by the MTT assay, which was in contrast to treatment with free DOX. The results indicated that only a small fraction of loaded DOX was released intracellular and the PCL fence could not be degraded by lipase in healthy cells. We then incubated H22 cells or HCT116 cells with TLND and treated the cells with SBY1. Cell death evaluated by trypan blue staining (Figure 2e and

Figure S7) indicated that SBY1 significantly promoted the cytotoxicity of TLND in both H22 cells and HCT116 cells; this was not due to the effect of SBY1 alone on the cells during 6 h of incubation, suggesting that differential DOX release from TLND was triggered by SBY1 bacteria and the release DOX subsequently killed the tumor cells.

SBY1 Bacteria and TLND Preferentially Distribute in the Tumor. We next analyzed the biodistribution of SBY1 bacteria in H22 tumor-bearing mice at different time points following intravenous injection of the bacteria. Bacterial burdens in blood, heart, liver, spleen, lung, and tumor were monitored. As shown in Figure 3a−c, SBY1 bacteria preferentially accumulated in tumors with a tumor-to-liver bacterial burden ratio of 610:1 at 3 days after SBY1 administration. Bacteria in the blood, heart, liver, spleen, and lung were gradually cleared over time and almost disappeared in those organs by day 7. Nevertheless, bacteria in the tumor did not significantly decrease over time, and the tumor-to-liver bacteria burden increased to 11291:1 and 2002:1 at 7 and 14 days, respectively. We also studied the biodistribution of bacteria SBY1 in the mesenteric lymph gland, left and right inguinal lymph nodes, and axillary lymph nodes. No bacteria in the lymph nodes was observed in 3, 7, and 14 days after SBY1 administration. These results suggest that injection of SBY1 bacteria provided a bacteria-accumulated artificial environment in the tumor.

On the other hand, the biodistribution of DOX was also evaluated in H22 tumor-bearing mice. TLND and DOX were administrated 7 days after bacteria injection when most of bacteria were cleared from endothelial organs but accumulated in the tumor. After 24 h, the tissues were collected, and DOX concentration was analyzed after thorough extraction from tissues according to the procedure that allowed full release of DOX from TLND. As shown in Figure 3d, in comparison to administration of free DOX at an equivalent dose at 10 mg per kilogram of body weight, a 6-fold higher DOX concentration was detected in tumors when TLND was administered 24 h after intravenous administration, owing to the EPR effect of TLND mediated by the abnormal tumor vasculature. It must be mentioned that administration of SBY1 bacteria did not significantly affect the biodistribution of drug in tumor and normal tissues (Supporting Information Figure S8).

TLND Differentially Releases DOX in SBY1-Infected Tumors. To investigate whether TLND differentially releases DOX in tumors with a bacteria-accumulated artificial environment after TLND accumulated in the tumor, we i.v. injected SBY1-GFP bacteria to H22 tumor-bearing mice, and after 7 days, TLND was i.v. injected. The distribution of DOX was analyzed from tissue sections of tumor and liver 24 h later. Figure 4 shows that SBY1-GFP preferentially accumulated in tumors but was cleared from the liver 7 days after injection. On the
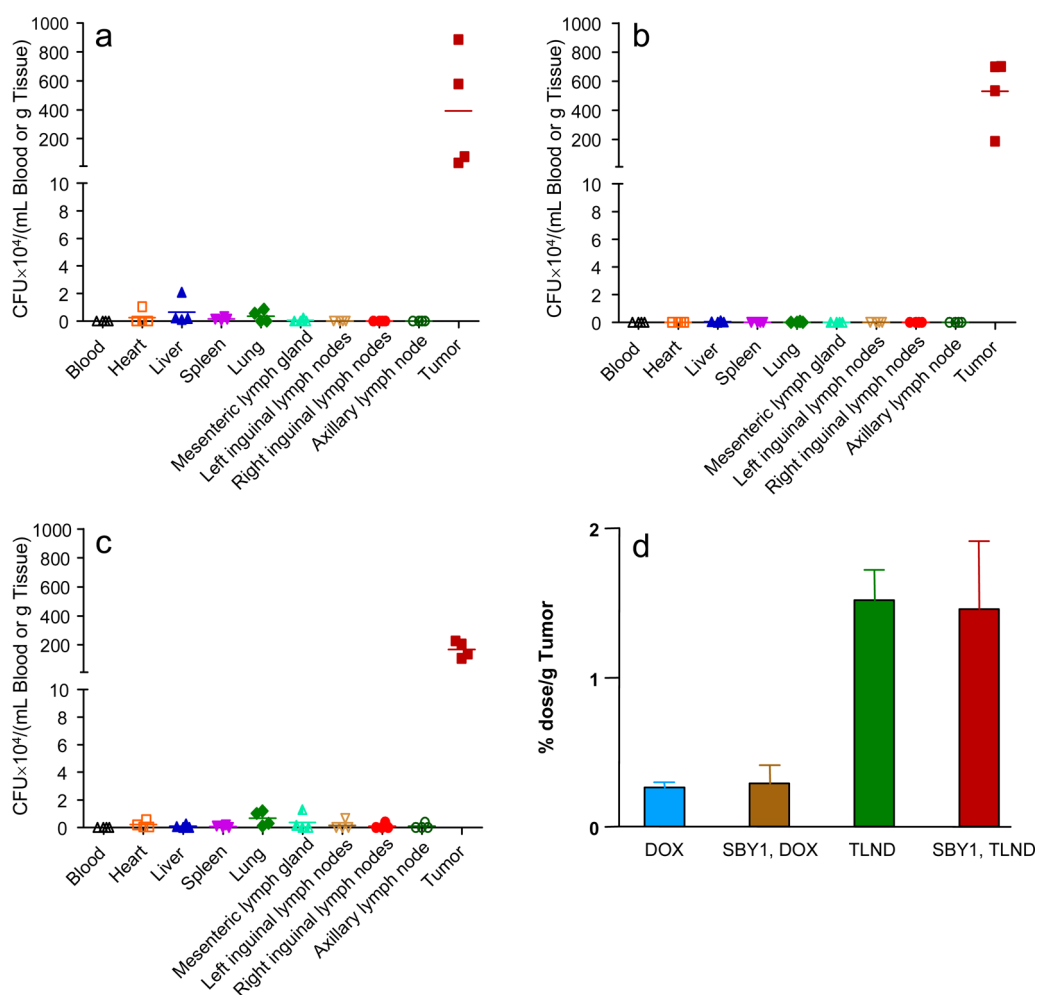
Figure 3. SBY1 and TLND preferentially distribute in tumors. (a—c) Bacterial burden in blood, heart, liver, spleen, lung, and tumor at 3 (a), 7 (b), and 14 days (c) after intravenous administration of SBY1 into H22 tumor-bearing mice; **(d)** amount of DOX in tumor with or without the administration of SBY1. The amount of DOX in tumor was measured by high-performance liquid chromatography. Means and standard deviations from four mice are shown (mean $\pm$ SD, $n = 4$).

other hand, TLND injection led to stronger fluorescence of DOX in tumors in comparison with free DOX injection, consistent with previous observations. More importantly, more fluorescence of DOX was localized in the nuclei of tumor cells if SBY1-GFP was administrated before the mouse received the TLND injection, strongly suggesting that SBY1-GFP in the tumor triggered DOX release from TLND. In addition, although the red fluorescence of DOX was observed in the liver of a mouse receiving TLND injections, the fluorescent signal was not localized in the cell nuclei, regardless of whether there was an SBY1-GFP injection, indicating that DOX might not be released from TLND in the liver. An extra image set in a different region is given in Figure S9. These results demonstrate that, following TLND accumulation in the tumor, DOX release in response to the bacteria-accumulated artificial environment in the tumor facilitated differential drug delivery to tumor cells.

SBY1 Bacteria Enhance the Anticancer Efficacy of TLND. The merit of differential DOX delivery by TLND to tumor

cells when combined with the bacteria-accumulated artificial environment was confirmed by the inhibition of tumor growth and the increased survival of mice. As shown in Figure 5, without SBY1 bacteria injection, the tumor continued to grow, and no significant inhibition of tumor growth was observed when H22 tumor-bearing mice received a single injection of free DOX or TLND at 5 mg per kilogram. Three injections of free DOX or TLND at the same doses did not inhibit HCT116 tumor growth either. The treatment of SBY1 alone exhibited obvious inhibition of tumor growth in both models in the initial stage, but the tumors regrew quickly after then, and the SBY1 treatment alone did not improve the survival of HCT116 tumor-bearing mice. The combination of TLND with SBY1 resulted in the prolonged regression of tumors. What's more, 90% of mice remained alive after 170 days when the mice were treated with TLND, which was significantly superior to the other treatments. From the weight change of tumor-bearing mice following SBY1 administration, a slight weight loss was observed in the first 7 days
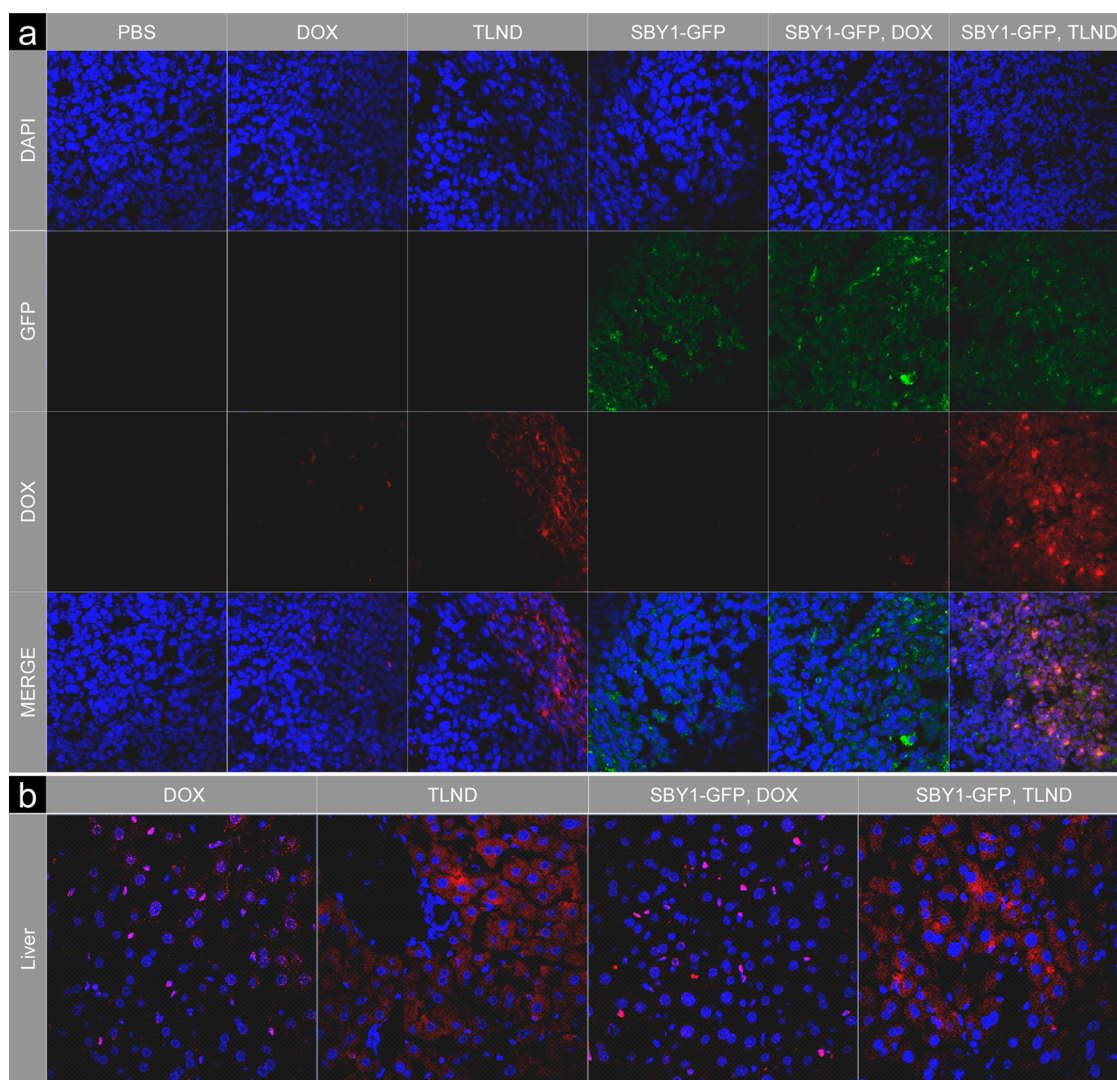
Figure 4. TLND differentially releases DOX in SBY1-infected tumors. SBY1-GFP (green) was administered to mice bearing H22 tumors, and after 7 days, DOX and TLND were injected intravenously at an equivalent dose of 10 mg of DOX per kilogram of body weight; the tissues were excised 24 h after drug administration. Confocal images were taken to investigate the distribution of DOX (red) in tissue sections from the tumor (a) and liver (b). DAPI (4′,6-diamidino-2-phenylindole, blue) was used to stain cell nuclei.

(Figure S10). Further TLND administration did not significantly decrease the weights of both H22-bearing mice and HCT116-bearing mice, while further injection of free DOX dramatically reduced the weights of mice. We have further investigated the potential toxicity of such treatment to the liver by analyzing the levels of alanine transaminase (ALT). As shown in Figure S11, no significant elevation was detected following the treatment.

In a separate experiment, the mice bearing H22 xenografts started out in two groups, treated with either SBY1 or PBS on day 15. The animals were then randomized into the treatment groups on day 22 and received DOX or TLND treatment. As shown in Figure S12, without SBY1 bacteria injection, the tumor continued to grow, and no significant inhibition of tumor growth was observed after administration of a single injection of free DOX or TLND at 5 mg per kilogram

mouse weight. The treatment of SBY1 alone exhibited obvious inhibition to tumor growth at the initial stage, but the tumors grew quickly after then. Combinational treatment of TLND and SBY1 resulted in prolonged regression of tumors. This result has also been demonstrated when the tumor weights were measured.

It should be mentioned that at day 1 and day 7 the expressions of immune factors TNFα, IL-6, and IFN-α in mice receiving SBY1 administration were all significantly higher when compared with that in mice receiving PBS injection (Figure S13). The phenomenon was found in both H22-bearing immunocompetent BALB/c mice and HCT116-bearing nude mice. The local inflammation in the liver and tumor was also analyzed using hematoxylin and eosin staining (H&E staining) in both H22-bearing mice and HCT116-bearing mice. As shown in Figure S14, administration of SBY1 did not induce
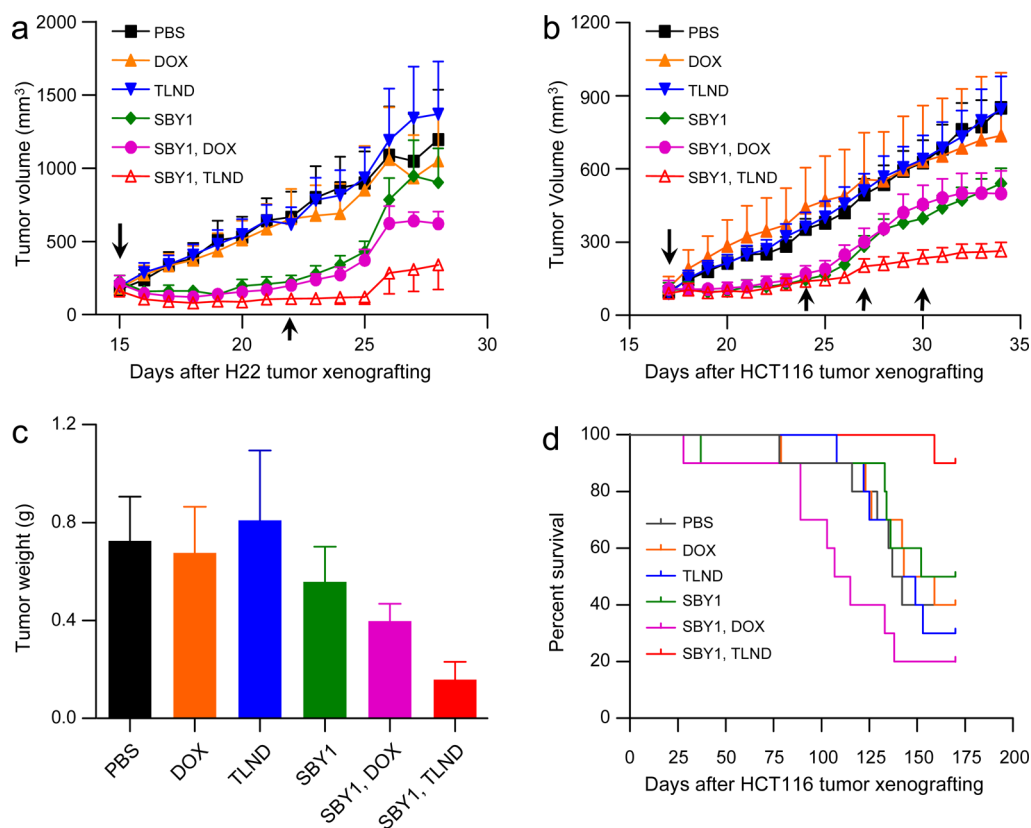
Figure 5. SBY1 treatment enhances the anticancer efficacy of TLND in mice. Tumor growth inhibition in BALB/c mice bearing H22 xenografts (a, $n = 5$, mean ± SEM) and nude mice bearing HCT116 human colorectal carcinoma xenografts (b, $n = 10$, mean ± SEM) after tail vein injection of different formulations; ↓ represents the intravenous administration of SBY1 at a dose of 3×10^7, and ↑ represents the intravenous administration of DOX or TLND at a dose of 5 mg of DOX per kilogram body weight. After treatment, the mice bearing H22 tumors were sacrificed and the tumors were collected and weighed (c), and the mice bearing HCT116 cancer xenografts were monitored to observe the survival rate (d). The differences between "SBY1, TLND" treatment group and all other groups were significant (P values were 0.013, 0.014, 0.004, 0.041, and 0.0007 for "PBS", "DOX", "TLND", "SBY1", and "SBY1, DOX" treatments, respectively, log-rank test) in the survival curves.

significant inflammation in the liver at day 1 and day 7 in both tumor models. Nevertheless, necrosis was found in the tumor at the same observation time after SBY1 administration, likely owing to the inflammatory reaction.[35−37]

CONCLUSIONS

In summary, we developed a new strategy for differential delivery of an anticancer drug, using bacteria-sensitive TLN as a drug carrier to selectively release drug in the bacteria-accumulated tumor. Taking SBY1 as the model bacterium, we successfully fabricated a unique bacteria-accumulated tumor artificial environment. Subsequent administrated TLND was thus selectively degraded in the bacteria-accumulated tumor environment, triggering differential doxorubicin release and selectively killing tumor cells. One of the encouraging observations in our study is that the combination of the bacteria-responsive TLND and SBY1 could theoretically increase the specificity and efficacy of an anticancer drug. The concept could easily be extended and improved by the combination of other tumor artificial environments and nanoparticles that are sensitive to the artificial environments.

MATERIALS AND METHODS

Materials. TLN was synthesized according to a procedure previously reported by us.[27] Agar A was obtained from Sangon Biotech (Shanghai) Co., Ltd. (China). Lipase from *Pseudomonas cepacia* and alkaline phosphatase (ALP) were obtained from Sigma-Aldrich Chemical Co. (USA). Bacto tryptic soy broth (TSB) was obtained from BD Biosciences (USA). The anticancer drug doxorubicin hydrochloride (DOX) was a product of Zhejiang Hisun Pharmaceutical Co, Ltd. All other solvents and reagents were used as received. An attenuated strain (*i.e.*, a methylthioadenosine/ *S*-adenosylhomocysteine nucleosidase mutant strain on the background of *Staphylococcus aureus* NCTC8325, named as SBY1) and green fluorescent protein expression SBY1 (SBY1-GFP) were kindly provided by Prof. Baolin Sun from the University of Science and Technology of China. The bacterial strain was grown in TSB at 37 °C with shaking, and then the bacteria were collected by centrifugation and then washed with PBS three times. Prior to the administration of the bacteria, the bacteria were then suspended in PBS with a concentration of about 1.5×10^8 CFU mL^{-1}, then 200 μL of the bacteria solution in PBS was injected into the tumor-bearing mice.

Cell Culture. The tumor cell lines H22 and HCT116 and human normal liver HL-7702 cells were cultured in Dulbecco's modified Eagle medium (DMEM, Gibco, Carlsbad, CA) with 10% fetal bovine serum (Gibco) at 37 °C with 5% CO_2.

Animals and Tumor Xenograft Model. Six to eight week old male BALB/c or female nude mice (from Vital River Laboratory Animal Technology Co. Ltd.) were implanted with subcutaneous injections of 3×10^6 H22 cells or 5×10^6 HCT116 cells, respectively. Tumor volume (mm³) was determined by measuring the length (*l*) and width (*w*) and calculated as $V = l \times w^2/2$. All animals received care in compliance with the guidelines outlined in the Guide for the Care and Use of Laboratory Animals. The procedures were approved by the University of Science and Technology of China Animal Care and Use Committee.

Drug Loading and Release. DOX was loaded into TLN by mixing TLN (60 mg) with DOX (6 mg) in DMSO at a DOX concentration of 50 mg mL^{-1} at 60 °C overnight. Water (12 mL) was then added dropwise. After 3 h of incubation at 60 °C, the mixture was placed at room temperature for 2 days. The DOX-loaded TLN was purified by dialysis (Spectra/Por 4, MWCO 12 000 to 14 000) against Milli-Q water for 1 day and ultrafiltrated with Millipore's Amicon Ultra-4 centrifugal filter (NMWL 100 kDa) to remove unloaded DOX which should be kept germ-free. The content of DOX loaded into TLN was calculated by subtracting the unloaded amount of DOX from the total amount used determined by high-performance liquid chromatography (HPLC), as described in the literature.[38]

The semisolid TSB-agar plate supplemented with TLND (0.125 mg mL^{-1} DOX) was prepared, on which 2 μL of SBY1-GFP culture was spotted, and was cultured at 37 °C. The fluorescent image acquisition of DOX and GFP was performed at different time intervals using a Xenogen IVIS Lumina system (Caliper Life Science, USA). Results were analyzed using Living Image 3.1 software (Caliper Life Sciences).

The release profiles of DOX from the TLND with or without *Pseudomonas* lipase (1 mg mL^{-1}) were studied at 37 °C in medium (Tris-HCl buffer, 0.01 mol L^{-1}, pH 7.4, containing 1 mM $MgCl_2$ and 50 mM KCl) using dialysis membrane tubing (Spectra/Por, Float-A-Lyzer, MWCO 12 000 to 14 000). At predetermined intervals, all the medium outside the tubing was collected to determine the amount of DOX released by HPLC, and fresh medium was provided. ALP (20 units L^{-1}) was added to the tubing at day 7.

H22 cells or HCT116 cells (1×10^5) were treated with PBS, SBY1 (1×10^6), TLND, or TLND plus SBY1 (1×10^6) with a DOX concentration of 0.5 μg mL^{-1}. After 3 h of incubation, cells were trypsinized, washed twice with PBS, and subjected to flow cytometric analysis.

Cytotoxicity. The relative cytotoxicity of the DOX or TLND was assessed with a methyl tetrazolium (MTT, Sigma-Aldrich Chemical Co.) viability assay against H22 cells, HCT116 cells, or HL-7702 cells according to the literature.[39] Briefly, the cells (1×10^5) were incubated with DOX or TLND at different concentrations for 24 h. The cell viability was normalized to that of cells cultured in complete culture medium.

The cell viability of H22 cells or HCT116 cells treated with PBS, SBY1, TLND, or TLND plus SBY1 was evaluated by trypan blue staining. Briefly, cells (50 000 cells per well in 24-well plate) were incubated with TLND at a concentration of DOX at 10 μg mL^{-1} for 18 h before the addition of SBY1 (5×10^5). After another 6 h of incubation, the cells were collected and suspended in 0.4% (w/v) trypan blue in PBS for 1 min that only stained dead cells, and then stained and unstained cells were counted on a hemocytometer.

Determination of the Biodistribution of SBY1 in Tumor-Bearing Mice. SBY1 bacteria, at a dose of 3×10^7 CFU, were administrated intravenously into H22 tumor-bearing mice. At different time intervals, mice were euthanized and the organs were harvested, weighed, and homogenized in sterile water. The number of viable bacteria per gram of organ was determined by plating serial dilutions of homogenized organs on TSB-agar culture medium and counting the colony forming units (CFU) of surviving bacteria.

Studies of the Biodistribution of Doxorubicin in Tumor-Bearing Mice. The biodistribution of DOX in the H22 tumor-bearing mice was

investigated according to the literature.[39] Briefly, DOX or TLND was administrated intravenously to mice with or without previous infection with SBY1 (3×10^7 CFU). The bacteria were intravenously injected 7 days before the administration of DOX or TLND with an equivalent DOX dose of 10 mg per kilogram of body weight. After 24 h, the tissue samples were harvested and weighed; the tissues were then dissolved in KH_2PO_4 solution (20 mM, pH 2.8) and homogenized with Ultra-Turrax T18 homogenizer (IKA, USA). Then, 200 μL of 10% (w/v) tissue homogenate was exposed to 50 μL of 5 M HCl at 50 °C for 1.5 h. After being cooled to room temperature, 50 μL of 1 M sodium hydroxide was added. The above mixture was subsequently extracted with chloroform/isopropyl alcohol (4:1, v/v) by vortex mixing for 1 min. Following centrifugation (10 000*g*, 5 min), the organic phase was collected and evaporated to dryness. The residue was then dissolved in 200 μL of mobile phase and centrifuged (10 000*g*, 5 min) to collect the supernatant for HPLC analysis. To generate the standard curve of DOX, the samples were prepared by adding free DOX to the tissues from untreated mice. The samples were treated and analyzed with the same approach as described above.

Confocal Laser Scanning Microscopy Studies of Distribution of SBY1 and DOX *in Vivo*. Seven days after the administration of SBY1-GFP (3×10^7 CFU), DOX and TLND were intravenously injected at an equivalent DOX dose of 10 mg per kilogram of body weight. The mice were sacrificed, and tissues including tumors and livers were collected after 24 h. The tissues were fixed in 4% paraformaldehyde overnight at 4 °C and then immersed overnight in a 30% sucrose solution. Tissues were then sequentially sectioned (10 μm thick) and counterstained with DAPI to indicate cell nuclei following the standard protocol of the manufacturer. The coverslips were mounted on glass microscope slides with a drop of antifade mounting media (Sigma-Aldrich Co., USA) to reduce fluorescence photobleaching. The images were taken under a laser scanning confocal microscope (LSM710Meta, Carl Zeiss Inc., Thornwood, NY).

Inhibition of Tumor Growth *in Vivo*. The tumor models with H22 and HCT116 xenografts were established as described above. The mice were treated with PBS or SBY1 (3×10^7 CFU), and after 1 week, DOX or TLND was intravenously administrated at an equivalent dose of 5 mg of DOX per kilogram of body weight. HCT116 tumor-bearing mice received three injections at an interval of 3 days of DOX or TLND 7 days after bacteria injection. Tumor growth was monitored by measuring the perpendicular diameter of the tumor using calipers. The survival of HCT116 tumor-bearing mice after treatment was assessed for 170 days after tumor implantation.

Statistical Analysis. Survival experiments were evaluated using the Kaplan–Meier method. Comparisons between curves were made using the log-rank test. Statistical analyses were performed using GraphPad Prism version 4.0. Statistical significance was assumed at a *P* value below 0.05.

Conflict of Interest: The authors declare no competing financial interest.

Supporting Information Available: Materials and methods, fluorescent intensity of DOX and TLND, diameter and count rate change of TLND upon incubation with lipase, quantification of DOX fluorescence of Figure 2a, lipase expression test, intracellular DOX fluorescence of HCT116 cells after the incubation with TLND without or with SBY1, cytotoxicity of DOX and TLND to cells, effect of SBY1 on the cytotoxicity of TLND to HCT116 tumor cells, and the biodistribution of DOX with and without the administration of SBY1, another image set for Figure 4, weight change of tumor-bearing mice after treatment, ALT level

after treatments, tumor growth inhibition in H22-bearing BALB/c mice, expression of immune factors following SBY1 administration, and the H&E straining of liver and tumor after the administration of SBY1. This material is available free of charge *via* the Internet at http://pubs.acs.org.

REFERENCES AND NOTES

1. LaVan, D. A.; McGuire, T.; Langer, R. Small-Scale Systems for *In Vivo* Drug Delivery. *Nat. Biotechnol.* **2003**, *21*, 1184–1191.
2. Springer, C. J.; Niculescu Duvaz, I. Antibody-Directed Enzyme Prodrug Therapy (ADEPT): A Review. *Adv. Drug Delivery Rev.* **1997**, *26*, 151–172.
3. Yeo, Y.; Gullotti, E. Extracellularly Activated Nanocarriers: A New Paradigm of Tumor Targeted Drug Delivery. *Mol. Pharmaceutics* **2009**, *6*, 1041–1051.
4. Slowing, I. I.; Vivero-Escoto, J. L.; Wu, C. W.; Lin, V. S. Y. Mesoporous Silica Nanoparticles as Controlled Release Drug Delivery and Gene Transfection Carriers. *Adv. Drug Delivery Rev.* **2008**, *60*, 1278–1288.
5. Du, J. Z.; Du, X. J.; Mao, C. Q.; Wang, J. Tailor-Made Dual pH-Sensitive Polymer-Doxorubicin Nanoparticles for Efficient Anticancer Drug Delivery. *J. Am. Chem. Soc.* **2011**, *133*, 17560–17563.
6. Fleige, E.; Quadir, M. A.; Haag, R. Stimuli-Responsive Polymeric Nanocarriers for the Controlled Transport of Active Compounds: Concepts and Applications. *Adv. Drug Delivery Rev.* **2012**, *64*, 866–884.
7. Zhu, L.; Kate, P.; Torchilin, V. P. Matrix Metalloprotease 2-Responsive Multifunctional Liposomal Nanocarrier for Enhanced Tumor Targeting. *ACS Nano* **2012**, *6*, 3491–3498.
8. Timko, B. P.; Dvir, T.; Kohane, D. S. Remotely Triggerable Drug Delivery Systems. *Adv. Mater.* **2010**, *22*, 4925–4943.
9. Ferris, D. P.; Zhao, Y. L.; Khashab, N. M.; Khatib, H. A.; Stoddart, J. F.; Zink, J. I. Light-Operated Mechanized Nanoparticles. *J. Am. Chem. Soc.* **2009**, *131*, 1686–1687.
10. Vivero-Escoto, J. L.; Slowing, I. I.; Wu, C. W.; Lin, V. S. Y. Photoinduced Intracellular Controlled Release Drug Delivery in Human Cells by Gold-Capped Mesoporous Silica Nanosphere. *J. Am. Chem. Soc.* **2009**, *131*, 3462–3463.
11. Kong, S. D.; Zhang, W. Z.; Lee, J. H.; Brammer, K.; Lal, R.; Karin, M.; Jin, S. H. Magnetically Vectored Nanocapsules for Tumor Penetration and Remotely Switchable On-Demand Drug Release. *Nano Lett.* **2010**, *10*, 5088–5092.
12. Mal, N. K.; Fujiwara, M.; Tanaka, Y. Photocontrolled Reversible Release of Guest Molecules from Coumarin-Modified Mesoporous Silica. *Nature* **2003**, *421*, 350–353.
13. Forbes, N. S. Engineering the Perfect (Bacterial) Cancer Therapy. *Nat. Rev. Cancer* **2010**, *10*, 784–793.
14. Arrach, N.; Cheng, P.; Zhao, M.; Santiviago, C. A.; Hoffman, R. M.; McClelland, M. High-Throughput Screening for Salmonella Avirulent Mutants That Retain Targeting of Solid Tumors. *Cancer Res.* **2010**, *70*, 2165–2170.
15. Pawelek, J. M.; Low, K. B.; Bermudes, D. Tumor-Targeted Salmonella as a Novel Anticancer Vector. *Cancer Res.* **1997**, *57*, 4537–4544.
16. Kawai, K.; Miyazaki, J.; Joraku, A.; Nishiyama, H.; Akaza, H. Bacillus Calmette−Guerin (BCG) Immunotherapy for Bladder Cancer: Current Understanding and Perspectives on Engineered BCG Vaccine. *Cancer Sci.* **2013**, *104*, 22–27.
17. Lamm, D. L. Bacillus Calmette−Guerin Immunotherapy for Bladder-Cancer. *J. Urol.* **1985**, *134*, 40–47.
18. Low, K. B.; Ittensohn, M.; Le, T.; Platt, J.; Sodi, S.; Amoss, M.; Ash, O.; Carmichael, E.; Chakraborty, A.; Fischer, J.; *et al.* Lipid A Mutant Salmonella with Suppressed Virulence and TNF Alpha Induction Retain Tumor-Targeting *in Vivo*. *Nat. Biotechnol.* **1999**, *17*, 37–41.
19. Saccheri, F.; Pozzi, C.; Avogadri, F.; Barozzi, S.; Faretta, M.; Fusi, P.; Rescigno, M. Bacteria-Induced Gap Junctions in Tumors Favor Antigen Cross-Presentation and Antitumor Immunity. *Sci. Transl. Med.* **2010**, *2*, 44ra57.
20. Cheong, I.; Huang, X.; Bettegowda, C.; Diaz, L. A.; Kinzler, K. W.; Zhou, S. B.; Vogelstein, B. A Bacterial Protein Enhances the Release and Efficacy of Liposomal Cancer Drugs. *Science* **2006**, *314*, 1308–1311.
21. Dang, L. H.; Bettegowda, C.; Huso, D. L.; Kinzler, K. W.; Vogelstein, B. Combination Bacteriolytic Therapy for the Treatment of Experimental Tumors. *Proc. Natl. Acad. Sci. U.S.A.* **2001**, *98*, 15155–15160.
22. Zhao, M.; Yang, M.; Ma, H. Y.; Li, X. M.; Tan, X. Y.; Li, S. K.; Yang, Z. J.; Hoffman, R. M. Targeted Therapy with a Salmonella Typhimurium Leucine-Arginine Auxotroph Cures Orthotopic Human Breast Tumors in Nude Mice. *Cancer Res.* **2006**, *66*, 7647–7652.
23. Sznol, M.; Lin, S. L.; Bermudes, D.; Zheng, L. M.; King, I. Use of Preferentially Replicating Bacteria for the Treatment of Cancer. *J. Clin. Invest.* **2000**, *105*, 1027–1030.
24. Yu, Y. A.; Shabahang, S.; Timiryasova, T. M.; Zhang, Q.; Beltz, R.; Gentschev, I.; Goebel, W.; Szalay, A. A. Visualization of Tumors and Metastases in Live Animals with Bacteria and Vaccinia Virus Encoding Light-Emitting Proteins. *Nat. Biotechnol.* **2004**, *22*, 313–320.
25. Diep, D. B.; Skaugen, M.; Salehian, Z.; Holo, H.; Nes, I. F. Common Mechanisms of Target Cell Recognition and Immunity for Class II Bacteriocins. *Proc. Natl. Acad. Sci. U.S.A.* **2007**, *104*, 2384–2389.
26. Yu, B.; Yang, M.; Shi, L.; Yao, Y. D.; Jiang, Q. Q.; Li, X. F.; Tang, L. H.; Zheng, B. J.; Yuen, K. Y.; Smith, D. K.; *et al.* Explicit Hypoxia Targeting with Tumor Suppression by Creating an "Obligate" Anaerobic Salmonella Typhimurium Strain. *Sci. Rep.* **2012**, *2*, 436.
27. Xiong, M. H.; Bao, Y.; Yang, X. Z.; Wang, Y. C.; Sun, B. L.; Wang, J. Lipase-Sensitive Polymeric Triple-Layered Nanogel for "On-Demand" Drug Delivery. *J. Am. Chem. Soc.* **2012**, *134*, 4355–4362.
28. Fang, J.; Nakamura, H.; Maeda, H. The EPR Effect: Unique Features of Tumor Blood Vessels for Drug Delivery, Factors Involved, and Limitations and Augmentation of the Effect. *Adv. Drug Delivery Rev.* **2011**, *63*, 136–151.
29. Bao, Y.; Li, Y.; Jiang, Q.; Zhao, L.; Xue, T.; Hu, B.; Sun, B. Methylthioadenosine/*S*-adenosylhomocysteine Nucleosidase (Pfs) of *Staphylococcus aureus* Is Essential for the Virulence Independent of LuxS/AI-2 System. *Int. J. Med. Microbiol.* **2013**, *303*, 190–200.
30. Chawla, J. S.; Amiji, M. M. Biodegradable Poly(ε-caprolactone) Nanoparticles for Tumor-Targeted Delivery of Tamoxifen. *Int. J. Pharm.* **2002**, *249*, 127–138.
31. Huang, C. F.; Cabot, M. C. Phorbol Diesters Stimulate the Accumulation of Phosphatidate, Phosphatidylethanol, and Diacylglycerol in 3 Cell-Types: Evidence for the Indirect Formation of Phosphatidylcholine-Derived Diacylglycerol by a Phospholipase-D Pathway and Direct Formation of Diacylglycerol by a Phospholipase-C Pathway. *J. Biol. Chem.* **1990**, *265*, 14858–14863.
32. Xiong, M. H.; Li, Y. J.; Bao, Y.; Yang, X. Z.; Hu, B.; Wang, J. Bacteria-Responsive Multifunctional Nanogel for Targeted Antibiotic Delivery. *Adv. Mater.* **2012**, *24*, 6175–6180.
33. Pandey, A.; Benjamin, S.; Soccol, C. R.; Nigam, P.; Krieger, N.; Soccol, V. T. The Realm of Microbial Lipases in Biotechnology. *Biotechnol. Appl. Biochem.* **1999**, *29*, 119–131.
34. Jaeger, K. E.; Ransac, S.; Dijkstra, B. W.; Colson, C.; Vanheuvel, M.; Misset, O. Bacterial Lipases. *FEMS Microbiol. Rev.* **1994**, *15*, 29–63.
35. Leschner, S.; Westphal, K.; Dietrich, N.; Viegas, N.; Jablonska, J.; Lyszkiewicz, M.; Lienenklaus, S.; Falk, W.; Gekara, N.; Loessner, H.; *et al.* Tumor Invasion of *Salmonella enterica* Serovar Typhimurium Is Accompanied by Strong Hemorrhage Promoted by TNF-alpha. *PLoS One* **2009**, *4*, e6692.
36. Weibel, S.; Stritzker, J.; Eck, M.; Goebel, W.; Szalay, A. A. Colonization of Experimental Murine Breast Tumours by *Escherichia coli* K-12 Significantly Alters the Tumour Microenvironment. *Cell. Microbiol.* **2008**, *10*, 1235–1248.
37. Westphal, K.; Leschner, S.; Jablonska, J.; Loessner, H.; Weiss, S. Containment of Tumor-Colonizing Bacteria by Host Neutrophils. *Cancer Res.* **2008**, *68*, 2952–2960.

38. Xiong, M. H.; Wu, J.; Wang, Y. C.; Li, L. S.; Liu, X. B.; Zhang, G. Z.; Yan, L. F.; Wang, J. Synthesis of PEG-Armed and Polyphosphoester Core-Cross-Linked Nanogel by One-Step Ring-Opening Polymerization. *Macromolecules* **2009**, *42*, 893–896.

39. Yuan, Y. Y.; Mao, C. Q.; Du, X. J.; Du, J. Z.; Wang, F.; Wang, J. Surface Charge Switchable Nanoparticles Based on Zwitterionic Polymer for Enhanced Drug Delivery to Tumor. *Adv. Mater.* **2012**, *24*, 5476–5480.